Exploring the Effect of Cyclization of Histamine H_1 Receptor Antagonists on Ligand Binding Kinetics

Zhiyong Wang,[#] Reggie Bosma,[#] Sebastiaan Kuhne,[#] Jelle van den Bor, Wrej Garabitian, Henry F. Vischer, Maikel Wijtmans, Rob Leurs, and Iwan J.P. de Esch*

Read Online

ACCESS | Metrics & More | Article Recommendations | Supporting Information

ABSTRACT: There is an increasing interest in guiding hit optimization by considering the target binding kinetics of ligands. However, compared to conventional structure−activity relationships, structure−kinetics relationships have not been as thoroughly explored, even for well-studied archetypical drug targets such as the histamine H_1 receptor (H_1R), a member of the family A G-protein coupled receptor. In this study, we show that the binding kinetics of H_1R antagonists at the H_1R is dependent on the cyclicity of both the aromatic head group and the amine moiety of H_1R ligands, the chemotypes that are characteristic for the first-generation H_1R antagonists. Fusing the two aromatic rings of H_1R ligands into one tricyclic aromatic head group prolongs the H_1R residence time for benchmark H_1R ligands as well as for tailored synthetic analogues. The effect of constraining the aromatic rings and the basic amines is systematically explored, leading to a coherent series and detailed discussions of structure−kinetics relationships. This study shows that cyclicity has a pronounced effect on the binding kinetics.
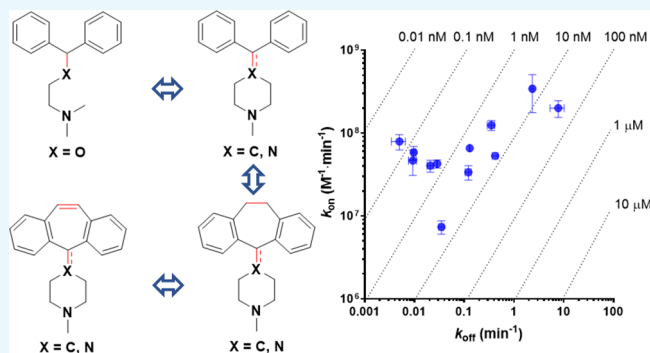
INTRODUCTION

The drug-target residence time (RT), defined as the reciprocal of the kinetic dissociation rate constant k_{off}, is increasingly acknowledged as an important metric for drug binding and is suggested to be linked to the *in vivo* efficacy of drugs.[1−4] In contrast, SAR-based hit and lead optimization programs often rely on the equilibrium dissociation constant (K_D) as a measure for the drug binding affinity. Often, the target binding kinetics of ligands are ignored, although there is not always a good correlation between the K_D and RT values of ligands for a drug target.[5,6] There is therefore a growing interest in understanding the molecular features that govern binding kinetics.[7−10] A study that used a Pfizer database containing mostly GPCR and kinase ligands suggests that molecular weight is one of the most important molecular properties that affects RT.[9] While other molecular properties play a less pronounced role in ligand dissociation, more lipophilic and more flexible compounds are suggested to have a higher probability of long RT.[9] Clearly, some of these descriptors are correlated and a study of focused (and smaller) series of compounds to explore particular molecular features like cyclicity would in our view be interesting. Tresadern *et al.* determined the RT of more than 1800 ligands for their binding to the dopamine D_2 receptor, showing that ligands with a long RT have, on average, a higher number of ring structures.[11] These findings suggest that the number of rotatable bonds[12]

and the number of rings can influence the drug-target RT. Other factors have also been correlated to RT, including the role of shielded hydrogen bonds between ligands and proteins that result in longer RT.[13]

For ligands targeting the archetypical and therapeutically relevant H_1R, several structural features have so far been shown to play a role in the binding kinetics. For example, the carboxylic acid group that is present in some of the second-generation H_1R antagonists can induce significantly slower binding kinetics, as was shown amongst others for levocetirizine (Figure 1).[6,15] However, the carboxylic acid moiety is necessarily not the only structural feature that plays an important role in the SKR of H_1R ligands. Also, for H_1R antagonists that lack this structural motif, major differences in binding kinetics have been observed. For example, it was shown that for some well-known tricyclic antihistamines like doxepin and desloratidine, the RT is considerably longer when compared to *e.g.*, mepyramine (Figure 1).[14,15] The aim of the
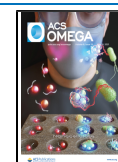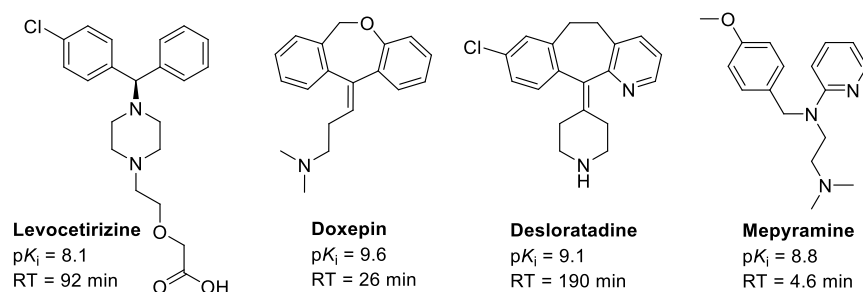
Figure 1. H$_1$R antagonists and their corresponding binding affinities (pK_i) and RT parameters. Values are taken from the literature.[14−18]
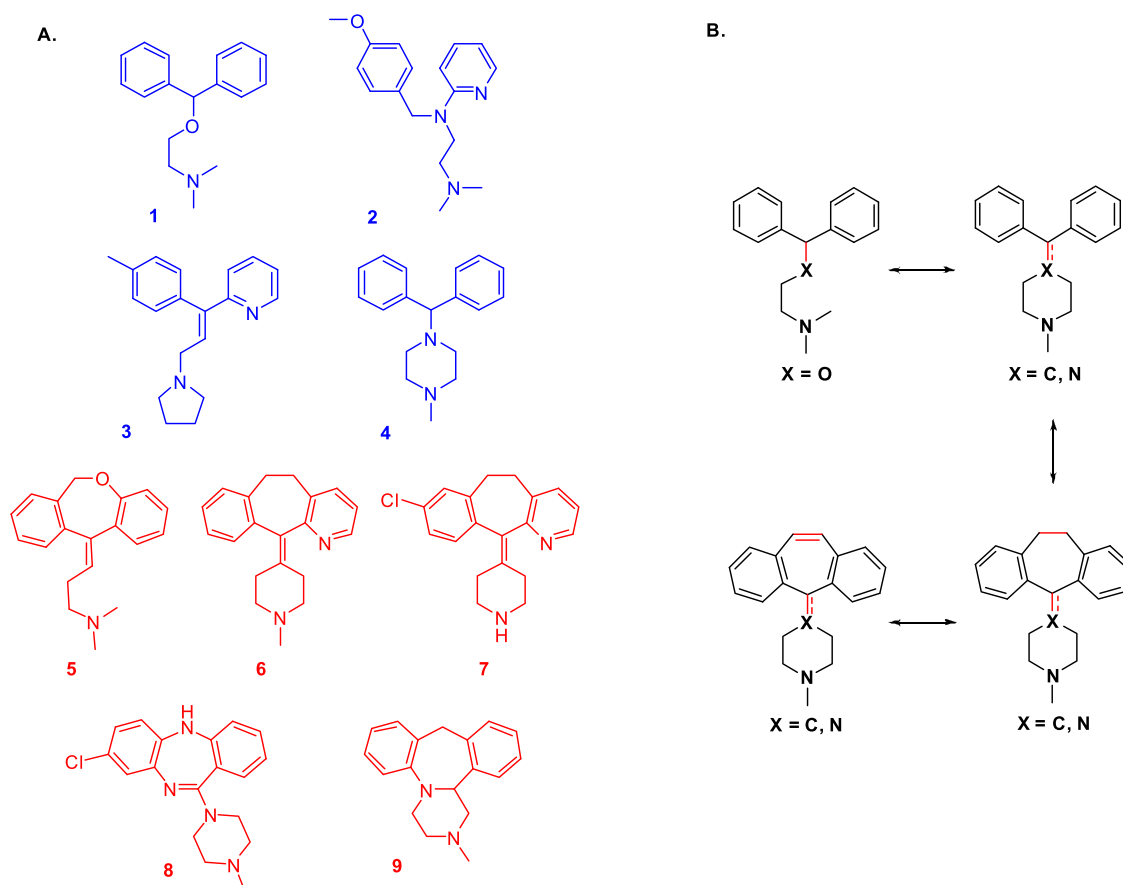
Figure 2. Structures of molecules. (A) Structures of benchmark H$_1$R ligands with comparable molecular weights classified as non-tricyclic (**1−4**, blue) and tricyclic (**5−9**, red) molecules (Table 1). (B) Design of a coherent set of ligands to explore the role of cyclicity (Table 2).
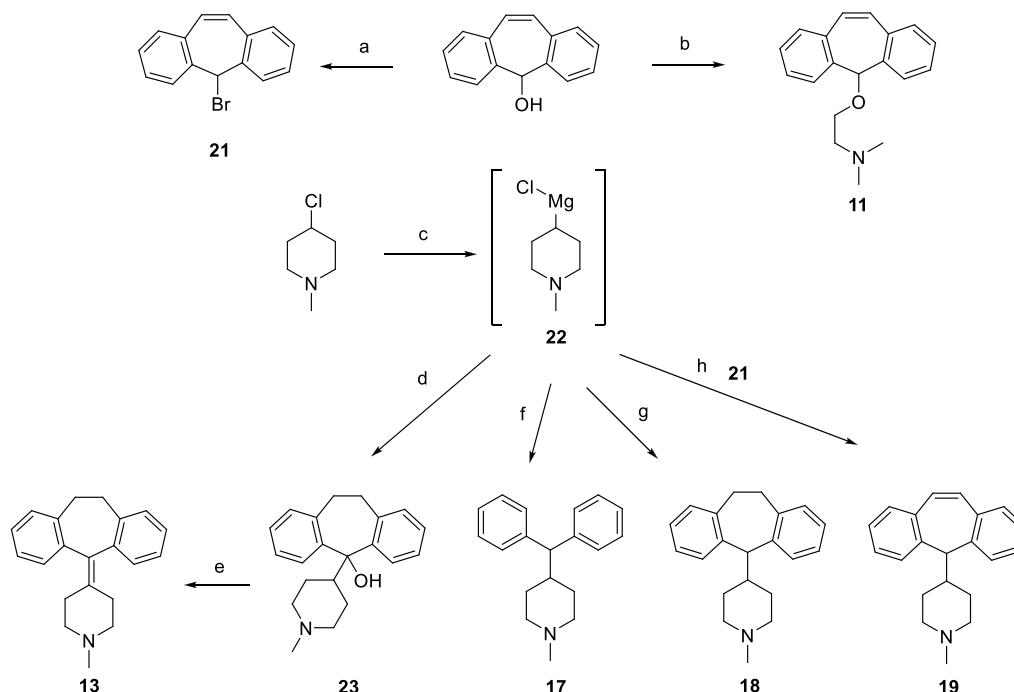
current study is to explore in a more systematic manner how cyclic systems influence ligand RT at the H$_1$R.

■ RESULTS

Selection of Benchmark H$_1$R Ligands. First, a set of known H$_1$R antagonists with similar size and a variety of ring systems was selected as benchmark ligands. The compounds all contain an aromatic head group and a basic amine, structural features that are characteristic for H$_1$R antihistamines.[19] Despite these similarities, *a priori* two groups of ligands can be distinguished, *i.e.*, the non-tricyclic ligands **1−4** and the tricyclic ligands **5−9** (Figure 2). These ligands result from different series and medicinal chemistry programs and have been optimized for affinity on a case to case basis, resulting amongst others in very specific substitution of the aromatic rings (*e.g.*, **2**, **3**, **7**, and **8**) and the incorporation of heteroatoms in the aromatic rings (*e.g.*, pyridine rings in **2**, **3**, **6**, and **7**).

Selection and Design of a Coherent Set of Tailored H$_1$R Ligands. A series of tailored synthetic derivatives (**10−19**) were designed that allows the stepwise comparison of ligands with nonfused aromatic ring systems with ligands in which these rings are linked by an ethyl or ethylene bridge (see Table 2 for structures). The series also varies the constraints of the linker connecting the aromatic moieties to the amine portion. Diphenhydramine (**1**) was selected as the starting point as it contains the prototypical basic amine and two separate phenyl groups (Figure 2). These aromatic rings were captured in a fused tricyclic system by using an ethyl linker to afford **10** or an ethylene linker to afford **11**. These modifications of the aromatic head groups were systematically applied to analogous ligands that incorporate the amine group of **1** into a variety of ring systems (that is, starting from **4**, **17**, and **12**). This includes replacing the sp^3 hybridized O atom in **1** with an sp^3 hybridized N (**4**) or C atom (**17**) or an sp^2

Scheme 1. Synthetic Approaches[a]

[a](a) CH$_3$COBr, EtOAc, reflux, 2 h, 46%. (b) N,N-dimethylaminoethanol, KOH, DMSO, rt., 24 h, 8%. (c) Mg (I$_2$/1,2-dibromoethane), THF, reflux, 1−2 h. (d) 10,11-Dihydro-5H-dibenzo[a,d][7]annulen-5-one, THF, rt., 15 h, reflux, 16% over two steps (incl. step c). (e) HCOOH, 100 °C, 2 h, 28%. (f) Bromodiphenylmethane, THF, rt., 4 h, 2% over two steps (incl. step c). (g) 5-Chloro-10,11-dihydro-5H-dibenzo[a,d][7]annulene, THF, 4 h, rt., 1% over two steps (incl. step c). (h) THF, rt., overnight, 2% over two steps (incl. step c).

Table 1. Kinetic Characterization of Binding of Benchmark Ligands at the H$_1$R[d]

Non-tricyclic ligands	Conformers[a]	pK_i	p$K_{D,calc}$[b]	k_{on} ($10^6 \cdot M^{-1} \cdot min^{-1}$)	k_{off} (min^{-1})	RT (min)[c]
1: diphenhydramine	52	8.0 ± 0.1	8.1 ± 0.2	300 ± 200	2.3 ± 0.2	0.43
2: mepyramine	20	8.8 ± 0.1	8.8 ± 0.1	150 ± 30	0.23 ± 0.03	4.4
3: triprolidine (Z)	26	8.3 ± 0.2	8.1 ± 0.1	40 ± 10	0.300 ± 0.035	3.1
4: cyclizine	13	8.2 ± 0.1	8.1 ± 0.0	53 ± 4	0.42 ± 0.06	2.4
Tricyclic ligands	Conformers[a]	pK_i	p$K_{D,calc}$[b]	k_{on} ($10^6 \cdot M^{-1} \cdot min^{-1}$)	k_{off} (min^{-1})	RT (min)[c]
5: doxepin	40	9.6 ± 0.1	9.1 ± 0.1	70 ± 10	0.060 ± 0.016	23
6: azatadine	12	10.2 ± 0.1	9.6 ± 0.0	32.0 ± 0.3	0.0088 ± 0.0001	114
7: desloratadine	8	9.1 ± 0.1	9.5 ± 0.1	18 ± 3	0.006 ± 0.001	170
8: clozapine	10	9.2 ± 0.1	9.3 ± 0.0	14.3 ± 0.3	0.0068 ± 0.0004	148
9: mianserin	26	9.4 ± 0.1	9.4 ± 0.0	55 ± 1	0.022 ± 0.002	45

[a]Number of conformers within 7 kcal/mol from the global energy minimum. [b]Calculated as k_{off}/k_{on}. [c]Calculated from the mean k_{off}: RT = $1/k_{off}$. [d]All values represent mean ± SEM of N ≥ 3.
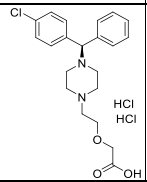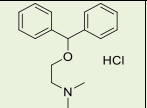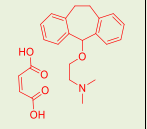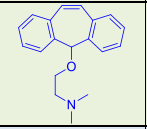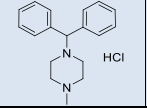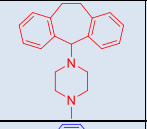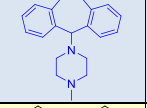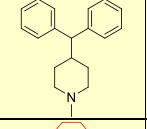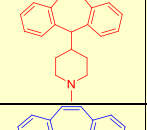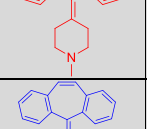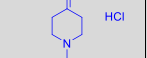
hybridized C atom (**12**). Bridging of the two aromatic rings in **4** and **17** and **12** as described for **1** affords three sets of analogs (**15**−**16**, **18**−**19**, and **13**−**14**, respectively).

Except for **18**, compounds **10**−**19** and associated synthetic routes are known in the peer reviewed literature[20−25] with some of those having been used in a histamine-receptor context. Some target compounds were available in-house (i.e., **10**, **12**, **14**, **15**, and **16**) as part of our compound collection. The remaining target compounds **11**, **13**, and **17**−**19** were synthesized from commercially available 4-chloro-1-methyl-piperidine and tricyclic alcohol 5H-dibenzo[a,d][7]annulen-5-ol (Scheme 1). The syntheses of **11** and **13** were conducted under conditions described in reports.[20,21] However, for **17**−**19**, we used the procedures described below. Compound **11** was made by addition of N,N-dimethylaminoethanol to 5H-dibenzo[a,d][7]annulen-5-ol,[26] while intermediate **21** was

obtained via bromination of the alcohol.[27] The key Grignard reagent **22** was synthesized via the reaction of the corresponding alkyl chloride with Mg.[28] Next, **22** was subjected in situ to different electrophiles to deliver compounds **17**−**19** and intermediate **23**. All these reactions proceeded in extremely low isolated yield (1−16%). We attribute this to the low reproducibility of the formation of **22** and of the required activation methods (such as I$_2$ and BrCH$_2$CH$_2$Br) as well as to the very challenging purification of the product mixtures due to high crystallinity. Dehydration of **23** in HCOOH afforded **13** in 28% yield.
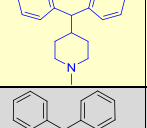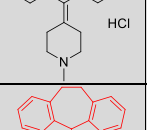
Conformational Analysis to Assess Flexibility. Conformational analysis was performed on all benchmark and tailored compounds to determine the number of conformers within 7 kcal/mol from the global energy minimum (Table 1 and Table 2) as a means to estimate the flexibility of the ligand.

Table 2. Characterization of Synthetic Ligands Binding at the H$_1$R[e]

#	Name	Structure[a]	Conformers[b]	pK_i	p$K_{D,calc}$[c]	k_{on} (10^6·M^{-1}·min^{-1})	k_{off} (min^{-1})	RT[d] (min)
20	Levocetirizine		N.D.	8.3 ± 0.1	8.1 ± 0.0	1.4 ± 0.2	0.011 ± 0.001	91
1	Diphenhydramine		52	8.0 ± 0.1	8.1 ± 0.2	300 ± 200	2.3 ± 0.2	0.43
10	VUFH1607		26	8.9 ± 0.0	8.7 ± 0.0	66 ± 3	0.129 ± 0.003	7.8
11	VUF16417		51	9.5 ± 0.1	9.7 ± 0.2	50 ± 20	0.009 ± 0.002	110
4	Cyclizine		13	8.2 ± 0.1	8.1 ± 0.0	53 ± 4	0.42 ± 0.06	2.4
15	VUFH1896		20	8.7 ± 0.1	8.4 ± 0.0	34 ± 7	0.12 ± 0.02	8
16	BS7617		9	8.7 ± 0.1	8.3 ± 0.1	7 ± 1	0.035 ± 0.004	29
17	VUF16290		14	7.6 ± 0.0	7.4 ± 0.1	200 ± 50	8 ± 2	0.13
18	VUF16416		28	9.2 ± 0.1	9.2 ± 0.0	43 ± 5	0.0285 ± 0.0004	35
19	VUF16327		5	9.3 ± 0.1	9.3 ± 0.0	40 ± 7	0.021 ± 0.003	48
12	VUF5577		11	8.5 ± 0.0	8.6 ± 0.0	120 ± 20	0.35 ± 0.06	2.9
13	VUF16217		12	9.6 ± 0.0	10.3 ± 0.1	80 ± 20	0.005 ± 0.002	200
14	Cyproheptadine		6	9.5 ± 0.1	9.8 ± 0.1	60 ± 10	0.010 ± 0.001	104

[a]Compound structures are shown in black for diphenyl moieties, in red for tricyclic structures with an ethyl linker, and in blue for tricyclic structures with an ethylene linker. [b]Number of conformers within 7 kcal/mol from the global energy minimum. [c]Calculated as k_{off}/k_{on}. [d]Calculated from the mean k_{off}: RT = 1/k_{off}. [e]All values represent mean ± SEM of $N \geq 3$.
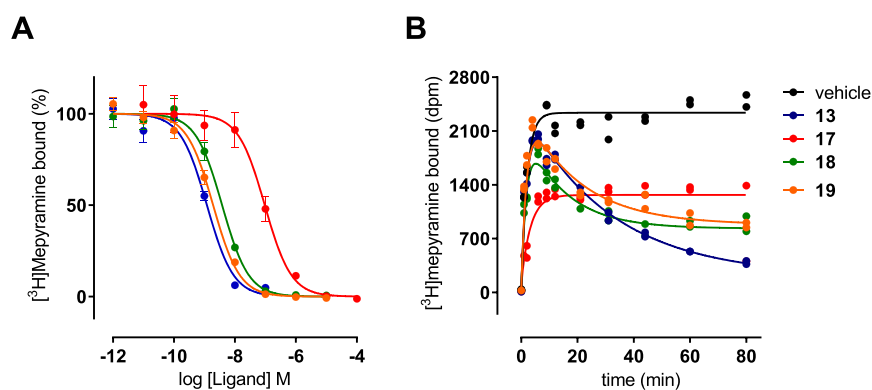
Figure 3. Radioligand binding in co-incubation with an exemplary set of compounds with varying rigidification elements. (A) [³H]mepyramine was co-incubated with increasing concentrations of **13** and **17–19** and the K_i value was determined from the resulting dose-dependent radioligand displacement by converting the observed IC_{50} value using the Cheng−Prusoff equation. (B) [³H]mepyramine binding was measured over time in the presence of approximately $10 \cdot K_i$ concentration of **13** and **17–19**. The kinetic association (k_{on}) and dissociation rate (k_{off}) constants were determined from the resulting radioligand binding kinetic traces. The shown representative graphs involve ≥3 experiments, depicting the mean and SEM of triplicate values (A) or the individual measurements with duplicate values per time point (B).

The stochastic search option within the Molecular Operating Environment (MOE) software package was used as this amongst others generates different conformations of the tricyclic ring systems.

Evaluation of the Benchmark Ligands. Binding affinity constants and kinetic parameters were determined using [³H]mepyramine radioligand binding studies with a homogenate of HEK293T cells transiently expressing the human H₁R, as described in the Experimental Section. Table 1 shows the affinities and kinetic parameters for all benchmark ligands. It was found that the tricyclic ligands **5−9** generally have a higher binding affinity (pK_i and $pK_{D,calc}$) and longer RT than the non-tricyclic ligands **1−4**. Among the tricyclic compounds was desloratadine (**7**), for which we confirm its long RT (previously reported as 190 ± 40 min).[14−17] Table 1 also shows the results of the conformational analyses. In general, it is noted that the number of identified conformers of a particular compound is significantly influenced by the number of distinct conformations that are identified for the aromatic ring systems. Distinct conformations of tricyclic rings cannot easily interconvert during energy minimizations, whereas the unconstrained aromatic ring systems are always minimized in the same conformation during the energy minimization step of the conformational analysis, and there clearly is a difference between the number of identified low energy conformers and the number of conformations that can easily be obtained, especially by the unconstrained non-tricyclic ligands.

Exploration of the Tricyclic Ring System and Linked Amine. The set of tailored synthetic derivatives (**10−19**) together with **1** and **4** was inspected in detail thereafter (Table 2). Affinity for the H₁R was determined by [³H]mepyramine displacement as depicted in Figure 3A for an exemplary set of compounds (**13** and **17−19**). A 100-fold difference in affinity was observed between **13** and **17**, whereas **18** and **19** both have affinities similar to **13**. Subsequently, the kinetic binding rate constants for binding to H₁R were determined in [³H]mepyramine competitive association binding assays, as originally described by Motulsky and Mahan.[29] The binding of 1−5 nM [³H]mepyramine in competition with an unlabeled ligand at a concentration amounting to approximately 10 times the K_i value of the latter was measured after different incubation times. Representative [³H]mepyramine association curves are shown in Figure 3B. In the presence and absence of

17, [³H]mepyramine binding to the H₁R gradually increases over time, indicating that **17** has a relatively short residence time (*i.e.*, comparable or shorter than that of [³H]-mepyramine).[18,30] In the presence of **13**, **18**, and **19**, however, initial overshoots are clearly observed (Figure 3B), indicating that these ligands have a longer RT as compared to [³H]mepyramine. Compounds **18** and **19** show a similar overshoot pattern, indicating that their k_{off} values are similar at the H₁R. In line with its high target-binding affinity, **13** shows the longest RT at the H₁R.

Table 2 shows the affinities and kinetic parameters as well as the results of the conformational analyses for all synthesized ligands. The conformational analyses afforded values in the same range as calculated for the benchmark ligands. For the biochemical assays, levocetirizine (**20**) was used as long-residence reference compounds, as it was in our earlier studies.[18,31] For clarity, the cell background colors in Table 2 indicate a classification of four series of ligands with the same basic amine element but varying connectivity of the aromatic rings to give triplets (**1**, **10**, **11/4**, **15**, **16/17**, **18**, **19/12**, **13**, **14**). The color coding of the compound structures indicates molecules with the same aromatic head group but with different amine elements (*e.g.*, red for compounds **10**, **13**, **15**, and **18** that all have a tricyclic ring with an ethyl linker).

Table 2 reveals that the systematic structural modifications have a pronounced effect on the binding kinetics. With the same unconstrained amine moiety, alteration of the aromatic rings by bridging **1** with an ethyl linker (to give **10**) results in a decrease of the dissociation rate constant (from 2.3 ± 0.2 to 0.129 ± 0.003 min⁻¹) and hence an 18-fold increase in RT at the H₁R. Replacing the ethyl linker of **10** with an ethylene linker causes an additional decrease in dissociation rate (k_{off} = 0.009 ± 0.002 min⁻¹ for **11**), *i.e.*, a 14-fold increase in RT, resulting in a long residence time of 110 min. Incorporating the aromatic rings in a tricyclic structure seems to lower the association rate constant, whereas the introduction of a double bond in the tricyclic ring does not seem to have a big additional effect (k_{on} = (300 ± 200) × 10⁶·M⁻¹·min⁻¹, (66 ± 3) × 10⁶·M⁻¹·min⁻¹, and (50 ± 20) × 10⁶·M⁻¹·min⁻¹ for **1**, **10**, and **11**, respectively). Within this triplet of **1**, **10**, and **11**, the binding affinity increases gradually with **11** having a pK_i of 9.5.
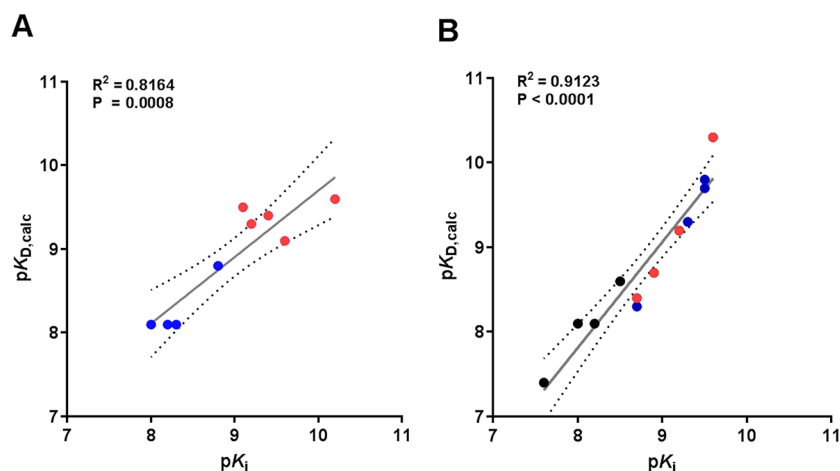
Figure 4. Affinity determined by radioligand displacement assay (pK_i) and the kinetic affinity ($pK_{D,calc}$). The lines represent linear regression of data. The two dashed lines indicate 95% confidence of the best-fit line. (A) Data for the reference compounds (Table 1). Blue dots represent the non-tricyclic compounds **1−4**, and the red dots represent the tricyclic compounds **5−9**. (B) Data for the coherent set of tailored H_1R ligands (Table 2). Black dots represent molecules that contain unconstrained diphenyl moieties, red dots are the tricyclic structures with an ethyl linker, and blue dots represent the tricyclic structures with an ethylene linker.
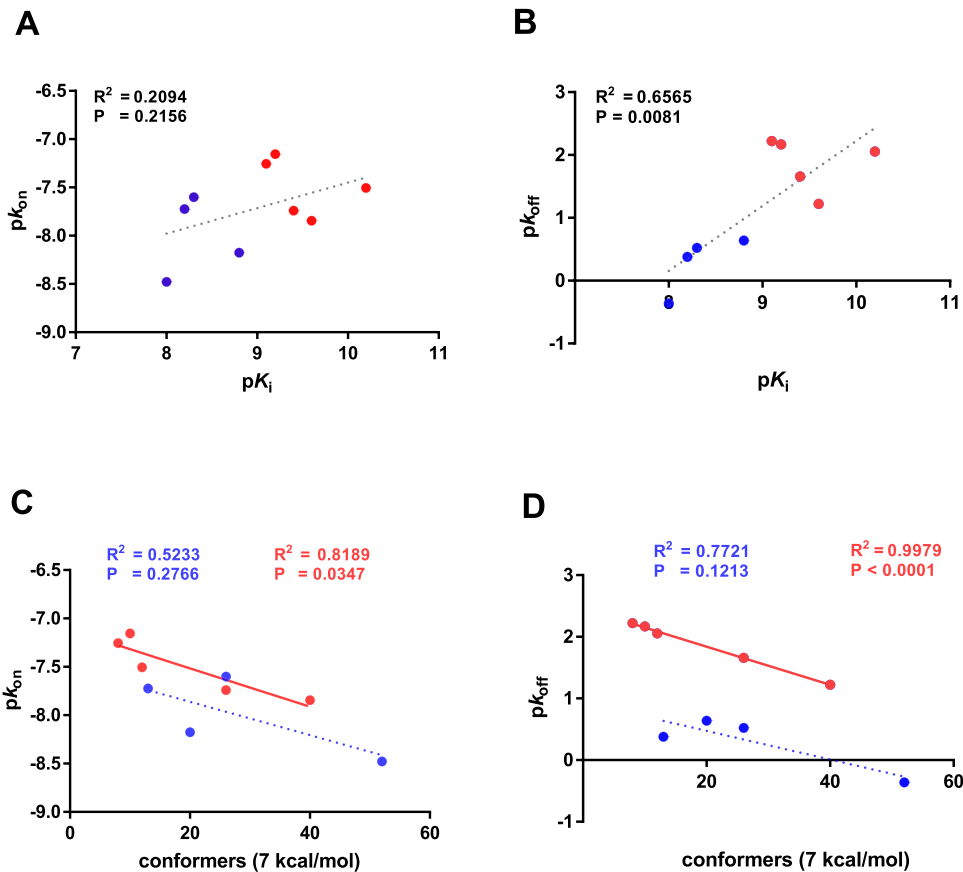
Figure 5. Exploring binding kinetics for the benchmark compounds. Blue dots represent the non-tricyclic compounds **1−4**, and the red dots represent the tricyclic compounds **5−9**. The lines represent linear regression of data. Solid lines indicate trends with an $R^2 > 0.80$, whereas dashed lines represent less convincing trends with $R^2 < 0.80$. (A) Negative logarithm of k_{on} (pk_{on}) and of the affinity (pK_i). (B) Negative logarithm of k_{off} (pk_{off}) and of the affinity (pK_i). (C) Negative logarithm of k_{on} (pk_{on}) and the number of conformers within 7 kcal/mol from the global energy minimum. (D) Negative logarithm of k_{off} (pk_{off}) and the number of conformers within 7 kcal/mol from the global energy minimum.

When bridging the two aromatic rings of the piperazine-containing structure of **4** with the ethyl and ethylene linker (leading to **15** and **16**, respectively), the residence time increases, although the differences are not as big as in the previous triplet (from 2.4 to 8 to 29 min for compounds **4**, **15**, and **16**, respectively). The association rate constants gradually get smaller, ($k_{on} = (53 \pm 4) \times 10^6 \cdot M^{-1} \cdot min^{-1}$, $(34 \pm 7) \times 10^6 \cdot M^{-1} \cdot min^{-1}$, and $(7 \pm 1) \times 10^6 \cdot M^{-1} \cdot min^{-1}$ for **4**, **15**, and **16**, respectively), with the tricyclic piperazine **16** having the slowest association of the three. Within this triplet, the binding

Figure 6. Exploring binding kinetics for the synthesized compounds. Molecules contain unconstrained diphenyl moieties (black dots), tricyclic structures with an ethyl linker (red dots), or tricyclic structures with an ethylene linker (blue dots), all c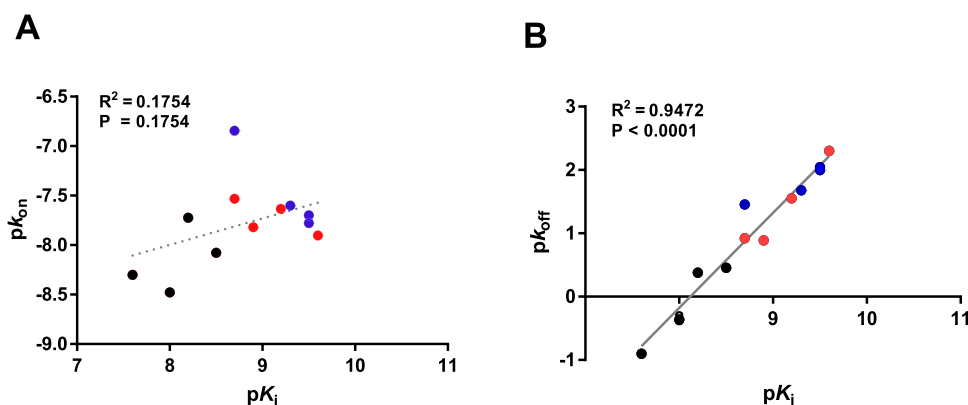ombined with four different amines (Table 2). The lines represent linear regression of data. Solid lines indicate trends with an $R^2 > 0.80$, whereas dashed lines represent less convincing trends with $R^2 < 0.80$. (A) Negative logarithm of k_{on} (pk_{on}) and of the affinity (pK_i). (B) Negative logarithm of k_{off} (pk_{off}) and of the affinity (pK_i).

affinity does not increase substantially and remains at a pK_i of 8.7 for both the tricyclic compounds **15** and **16**.

Within the piperidine-containing triplet **17**, **18**, and **19**, a large 270-fold increase in RT is observed when connecting the aromatic rings of **17** (RT = 0.13 min) to the tricyclic **18** (RT = 35 min). Introducing a double bond in the linker (**19**) results in a similar increase in the RT (RT = 48 min). This latter modification does not seem to alter k_{on} ((43 ± 5) × $10^6 \cdot M^{-1} \cdot min^{-1}$ and (40 ± 7) × $10^6 \cdot M^{-1} \cdot min^{-1}$ for **18** and **19**, respectively).

Interestingly, when evaluating the triplet of constrained piperidines **12**, **13**, and **14**, the ethyl-bridged compound **13** has the longest RT within the triplet (RT = 200 min) and one of the longest RT values in this study, even compared to the benchmark compounds presented in Table 1. Introducing a double bond in the linker, leading to **14** (cyproheptadine), in this case affords a slightly shorter residence time (RT = 104 min). The association rate constants seem to gradually get smaller (k_{on} = (120 ± 20) × $10^6 \cdot M^{-1} \cdot min^{-1}$, ($80 \pm 20$) × $10^6 \cdot M^{-1} \cdot min^{-1}$, and ($60 \pm 10$) × $10^6 \cdot M^{-1} \cdot min^{-1}$ for **12**, **13**, and **14**, respectively) and the binding affinities for **13** and **14** remain equally high (pK_i = 9.6 and pK_i = 9.5, respectively).

It is noted that the binding affinities (pK_i) determined in equilibrium radioligand displacement experiments and the $pK_{D,calc}$ values derived from radioligand competitive association assays ($K_{D,calc} = k_{off}/k_{on}$) experiments correlate well (Figure 4A,B for the reference compounds and for the set of tailored H_1R ligands, respectively), giving confidence in the accuracy of the measured binding rate constants.

■ DISCUSSION

For several decades, H_1R antagonists have been successfully used in the clinic for treating symptoms of allergic diseases,[32−34] and more recently, they have also been applied to regulate sleep-wakefulness.[35−37] As such, structure−activity relationships of H_1R antagonists have been studied intensively. Hallmark features of H_1R ligands include aromatic rings arranged in a diphenyl or tricyclic structure. Another typical feature is the basic amine that is either flexible or captured in an aliphatic heterocyclic ring. Other ligands are equipped with a carboxylic acid moiety to regulate pharmacokinetic properties and prevent brain penetration of the ligands. It has been shown by us and others[6] that these features also have a remarkable effect on binding kinetics. Here, we have focused on the

structure−kinetics relationships associated with the aromatic rings and amine moieties.

For the selected benchmark compounds **1−9**, plotting pK_i against pk_{on} (Figure 5A) and pk_{off} (Figure 5B) indicates that there is no clear trend between pK_i and the association rate constant, whereas there is a moderate but significant correlation between the affinity and the dissociation rate constant. These results are in line with recent findings for adenosine A_3 receptor antagonists,[38] whereas a series of A_3 agonists showed a better correlation between the affinity and the association rate.[39] A recent study exploring the binding kinetics of histamine H_3R reference ligands showed a better correlation between the affinity and the association,[40] illustrating that the relationships between affinity and binding kinetics vary with receptors and compounds (series dependent). For the compounds in Table 1, all tricyclic ligands have a lower dissociation rate k_{off} (longer RT) than the non-tricyclic ligands. The differences between non-tricyclic ligands **1−4** and tricyclic ligands **5−9** were further explored by conformational analysis. The number of conformers within an energy window of 7 kcal/mol from the global energy conformation was determined (Table 1). Figure 5 shows the number of conformations plotted against pk_{on} (Figure 5C) and pk_{off} (Figure 5D). While the ligands studied represent a very focused series to systematically explore cyclicity, it is noted that the number of compounds in this analysis is limited. Nevertheless, a trend line across the non-tricyclic compounds (blue dots) appears significantly lower than a trend line across the tricyclic compounds (red dots), not only suggesting a correlation between residence times and number of conformers but also indicating an additional, unidentified feature (that is not captured by the conformational analysis) that distinguishes the non-tricyclic from the tricyclic compounds.

The series of tailored compounds (Table 2) that was synthesized to explore the SAR and SKR of the tricyclic ring systems and basic amines confirms the observations made for the benchmark H_1R antagonists (Table 1), namely, that the ring systems have a pronounced effect on the binding kinetics. In all cases, linking the two aromatic rings into tricyclic systems leads to a longer residence time and higher affinity. Introducing a double bond in the linker that connects the aromatic rings (leading to compounds **11**, **16**, **19**, and **14**) often results in the compounds with the longest residence time within the triplets. A notable exception to the latter is **14**, as in the triplet with the
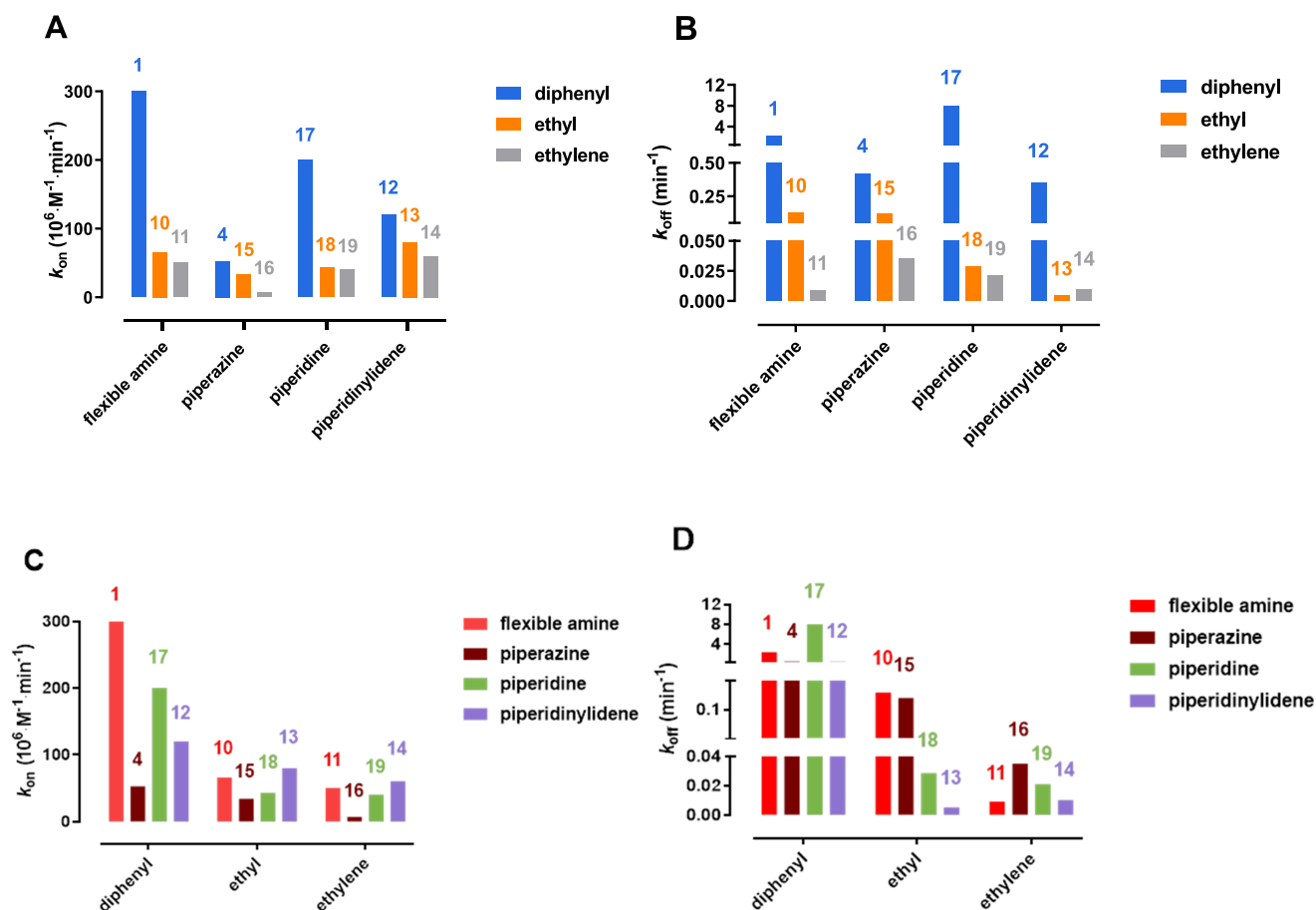
Figure 7. SKRs exploring the role of the different ring systems. (A) Association rate constants organized by aromatic ring systems. (B) Dissociation rate constants organized by aromatic ring systems. The same data can be rearranged to focus on basic amines: (C) Association rate constants organized by basic amines. (D) Dissociation rate constants organized by basic amines. The numbers above the bar correspond to the respective molecule numbers.

constrained piperidine moiety (*i.e.*, **12**−**14**), it is the tricyclic compound with the ethyl linker (**13**) that has the longest RT. The residence time of **13** (RT = 200 min) is amongst the longest of the synthesized compounds (Table 2) and the studied benchmark compounds (Table 1).

When plotting pKi versus pk_{on} and pk_{off} (Figure 6A,B, respectively), it appears that the dissociation rate constants, but not the association rate constants, are correlated to the binding affinity, a finding that seems even more pronounced than that observed for the benchmark compounds in Table 1 and Figure 5A,B. As shown in Figure 6B, compounds that contain two unconstrained aromatic rings (black dots; **1**, **4**, **17**, and **12**) have lower affinity and faster unbinding. The tricyclic compounds with an ethyl linker (red dots; **10**, **15**, **18**, and **13**) and the tricyclic compounds with an ethylene linker (blue dots; **11**, **16**, **19**, and **14**) have higher affinity and slower unbinding. A similar correlation cannot be observed for association rate constants (Figure 6A).

The compounds in Table 2 were also subjected to conformational analysis. However, in contrast to the benchmark compounds listed in Table 1, no trends are observed between the number of conformers and the binding kinetics (Figure S1, Supporting Information). It is noted that the number of conformers is significantly influenced by the number of distinct conformations of the aromatic rings that are identified by the search algorithm. Bridging the aromatic

rings leads to very different conformations of the tricyclic ring system that cannot easily interconvert, whereas the unconstrained aromatic rings of **1**, **4**, **17**, and **12** are always minimized in the same relative conformation during the energy minimization step of the conformational analysis. Clearly, the non-tricyclic ligands can easily adjust the orientation of their unconstrained aromatic rings to adopt a slightly different binding conformation. The possibility that ligands can bind in an energy conformation that is somewhat higher than one of the identified conformers might be more important for the series of tailored (unoptimized) compounds presented in Table 2 than for the optimized benchmark compounds represented in Table 1. The compounds from Table 2 are designed to allow pairwise comparisons of the tricyclic ring systems and different basic amines but are not fully optimized for binding to the H_1R. The benchmark compounds of Table 1 represent the best compounds within a ligand series that are highly fine-tuned for an ensemble of properties, not only binding affinity but also other factors such as pharmacokinetic and selectivity profiles (the different substitution patterns on the aromatic rings of the benchmark compounds illustrate this aspect).

The dataset represented in Table 2 allows for a careful deduction of SKRs, especially with respect to the effect of the structural elements in the compounds. As indicated earlier, capturing the unconstrained diphenyl rings into a tricyclic

structure leads to lower association rate constants for every amine moiety explored (*i.e.*, flexible amine, piperazine, piperidine, and piperidinylidene; see Figure 7A). In the case of the flexible amines (**1**, **10**, and **11**), capturing the aromatic rings in a tricyclic system has a large effect on the association rate constants. In contrast, the differences in k_{on} are rather small if the constrained piperidinylidene is used as a basic moiety (**12**, **13**, and **14**). In all cases, the tricyclic derivative with the ethylene linker has the lowest association rate constant within the triplet, but only for the derivative in the piperazine series (*i.e.*, **16**, $k_{on} = (7 \pm 1) \times 10^6 \cdot M^{-1} \cdot min^{-1}$), the association rate constant seems to be substantially lower than its analog with the ethyl linker (**15**, $k_{on} = (34 \pm 7) \times 10^6 \cdot M^{-1} \cdot min^{-1}$).

The influence on the dissociation rate constants (Figure 7B) is more pronounced, with the tricyclic compounds having a much smaller k_{off} value, *i.e.*, longer residence time. For the flexible amines (**1**, **10**, and **11**) and the piperazine-containing compounds (**4**, **15**, and **16**), a clear difference is seen between the tricyclic compounds that contain an ethyl linker and the ethylene linker, the latter tricyclic ring system leading to the compounds with the slowest dissociation (longest RT). For the piperidine-containing compounds, there is no significant difference in dissociation rate constants for the two tricyclic compounds **18** and **19**. For the piperidinylidene-containing compounds, the tricyclic compounds also have very low dissociation rate constants (long RT), with the tricyclic compound with an ethyl linker (*i.e.*, **13**) having a remarkable slow dissociation ($k_{off} = 0.005$ min^{-1}).

Using the same data but focusing the SKR discussions on the different amine moieties (*i.e.*, flexible amine, piperazine, piperidine, and piperidinylidene), it can be seen that the piperazine moiety consistently has the slowest association for the quartets that contain the same aromatic ring systems (Figure 7C). Also, in this representation of the data, **16** is noted for having a particularly fast association or lower association constant. The effect of different amines on the dissociation rate constants (Figure 7D) is less pronounced than the effect of the aromatic ring systems (Figure 7A, B). No consistent pattern is observed for the different quartets, meaning that the effect of exchanging the basic moieties is difficult to predict. For the ethylene-linked tricyclic series, it is noted that the aforementioned piperazine **16** has the fastest unbinding.

Representing the same binding kinetic data of Table 2 in an isoaffinity kinetic plot (Figure 8) clearly illustrates that restraining the diphenyl moieties into tricyclic rings leads to higher affinity, an effect that is mainly caused by decreasing dissociation rate constants (consider the trend observed for squares **1**, **10**, and **11**; diamonds **12**, **13**, and **14**; and inverted triangles **17**, **18**, and **19**). For the piperazine-containing compounds (triangles **4**, **15**, and **16**), the changes in association and dissociation are more balanced, resulting in compounds with similar affinities ($pK_{D,calc} = 8.1$, 8.4, and 8.3, respectively), as indicated in the plot by the three triangles that stay close to the same isoaffinity diagonal. The molecular reason for this is not clear. The amine moieties of all these ligands are expected to bind to the aspartic acid residue D3.32, a hallmark anchoring point in aminergic GPCRs that is known to bind the amine groups of the endogenous agonists and also to amine-containing ligands. As the piperazine ring contains a second basic nitrogen atom, it can be speculated that this feature facilitates the breaking of that key hydrogen bonding as
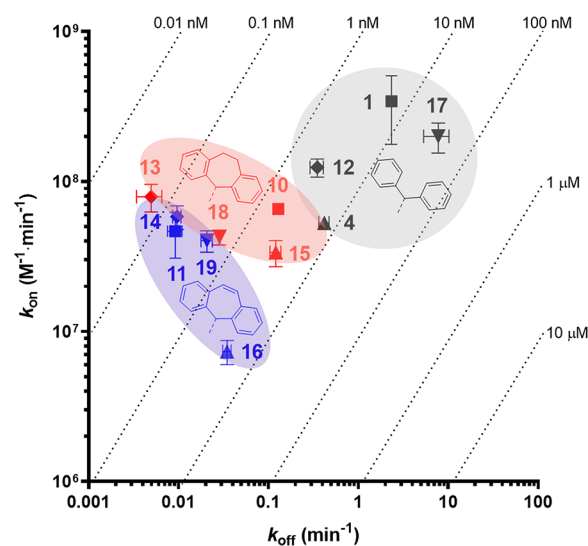

Figure 8. Two-dimensional isoaffinity kinetic plot indicating k_{on}, k_{off}, and $K_{D,calc}$ values (diagonal lines). The colored molecule numbers, symbols, and zones indicate the particular aromatic ring systems and correspond to the color coding used in Table 2 (black: no bridge, red: ethyl bridge, and blue: ethylene bridge). Symbols correspond to flexible amines (squares), piperazines (triangles), piperidines (inverted triangles), and piperidinylidenes (diamonds).

in an anchimeric assistance, resulting in a shorter residence time.

In conclusion, it was shown in this study that a tricyclic ring system increases affinity and RT at the H$_1$R. The increase in affinity is mainly achieved by changes in dissociation rate constants. The influence of the basic amine moiety on the binding kinetics appears less pronounced, although for the piperazine-containing compounds, the changes in dissociation and association rate constants are more balanced, resulting in compounds with similar affinity. While the effect of the tricyclic ring systems on the binding kinetics is very pronounced, analysis of well-studied benchmark compounds suggests that the effect of rigidification of the aromatic ring system on affinity and residence time can be further optimized by careful optimization of the tricyclic moiety, for example, by decoration of the aromatic rings. More broadly, our study shows that certain effects of variations in small-molecule structure on k_{off} and k_{on} profiles of protein binding can be identified but are as of yet expected to not be straightforward to predict for any scaffold−protein pair. We recommend that these relationships are carefully studied for various scaffolds and protein targets as any emerging general trends could facilitate the design of effective drugs.

■ EXPERIMENTAL SECTION

Pharmacology. Dulbecco's Modified Eagle's Medium was acquired from Sigma Aldrich (St. Louis, MO, USA). Medium was supplemented with fetal bovine serum and penicillin/streptomycin from GE healthcare (Uppsala, Sweden). Linear polyethylenimine (25 kDa) was acquired from Polysciences (Warrington, PA, USA). HBSS, trypsin, and the BCA protein assay were bought from Thermo Fischer Scientific (Waltham, MA, USA). The Branson sonifer 250 homogenizer was bought from Emerson (St. Louis, MO, USA). GF/C plates, Microscint-O, [3H]mepyramine, the cell harvester, and the Wallac Microbeta counter were all bought from Perkin Elmer

(Waltham, MA, USA). Diphenhydramine hydrochloride was purchased from Sigma Aldrich. Mepyramine maleate was obtained from Research Biochemicals International. Triprolidine hydrochloride was purchased from Tocris. Azatadine dimaleate and desloratadine were purchased from HaiHang Industry Co., Ltd. Cyclizine hydrochloride was purchased from Toronto Research Chemicals (TRC). Stock solutions of H_1R binding compounds were made at 10 mM in DMSO and were further diluted to a final concentration of ≤1% DMSO in binding experiments.

Cell Culture and Radioligand Binding. Cell maintenance, production of cell homogenates expressing the HA-H_1R, and the performed radioligand binding experiments were previously described and adapted with minor changes.[14] In short, HEK293T cells were transiently transfected using 25 kDa polyethylenimine with a pcDEF3 vector encoding the N-terminally HA tagged H_1R. Cells were collected and frozen 2 days post-transfection. Upon conducting a radioligand binding experiment, a frozen aliquot of cells was reconstituted in binding buffer (50 mM Na_2HPO_4/KH_2PO_4, pH 7.4), homogenized, and then co-incubated (0.5−3 μg protein content per well) with [^{3}H]mepyramine (1−5 nM) with or without an additional unlabeled ligand at 25 °C under gentle agitation. Binding reactions were terminated by filtration and three rapid consecutive wash steps using ice-cold wash buffer (50 mM Tris-HCl, pH 7.4). Filter-bound radioactivity was quantified by scintillation counting using the Wallac Microbeta.

Competitive Association Assay. Previously, it was determined for the radioligand [^{3}H]mepyramine binding the H_1R, that the equilibrium dissociation constant (K_D) is 2.29 nM, the kinetic dissociation rate constant (k_{off}) is 0.22 min^{-1}, and the kinetic association rate constant (k_{on}) is 1.1×10^8·min^{-1}·M^{-1}.[14] In radioligand displacement experiments, a single concentration 1−5 nM [^{3}H]mepyramine was co-incubated with increasing concentrations (10^{-12} to 10^{-4} M) of unlabeled ligands for 4 h at 25 °C. K_i values could be determined from the displacement curves by converting the obtained IC_{50} values using Cheng−Prusoff equation.[41] For competitive association experiments, a single concentration 1−5 nM [^{3}H]mepyramine was co-incubated with a single concentration unlabeled ligand for increasing incubation times of 0−80 min at 25 °C. The concentration of the antagonist was chosen to be 10·K_i, or fine-tuned to have a similar level of radioligand displacement after 80 min (>40%). Kinetic binding rate constants of the unlabeled ligands were determined from the resulting radioligand binding over time by fitting the data to the Motulsky and Mahan model using nonlinear regression.[29] In this model, the concentrations of both ligands and the k_{on} and k_{off} of [^{3}H]mepyramine at the H_1R were constrained (see above). From the fitted kinetic binding rate constants, the equilibrium dissociation constant ($pK_{D,calc}$) and residence time (RT) could be calculated.

Calculations. SMILES for compounds **1−19** were obtained from ChemBioDraw Ultra (version 16.0.1.4) and protonated according to the protonate 3D module (default settings). Conformational analyses were performed in MOE2016.08 using a stochastic search algorithm. Under the same energy windows of 7 kcal/mol, a stochastic search produces conformations by stochastically perturing structures. The rejection limit was increased to 1000 in order to find all possible conformers. Double bonds were allowed to rotate during sampling. The sp^3 stereocenters were allowed to invert

in the case of nitrogen atoms (*e.g.*, mepyramine). Ring conformations other than chair were accepted. Unique conformations (within 0.25 RMSD limit) were stored and counted.

Chemistry. *General Remarks.* Anhydrous THF, CH_2Cl_2, DMF, and Et_2O were obtained by elution through an activated alumina column from Inert PureSolv MD5 before use. Diphenhydramine hydrochloride (**1**) was obtained from Sigma Aldrich, levocetirizine dihydrochloride (**20**) was obtained from Biotrend, cyclizine hydrochloride (**4**) was obtained from Toronto Research Chemicals Inc., doxepin hydrochloride (**5**) was obtained from Tocris, and clozapine (**8**) was obtained from TCI. Compounds **10**, **12**, **15**, and **16** as well as mianserin (**9**) and cyproheptadine hydrochloride (**14**) were gifts from Gist Brocades (The Netherlands). All other solvents and chemicals were acquired from commercial suppliers and were used without further purification. ChemDraw professional 16.0 was used to generate systematic names for all molecules. All reactions were performed under an inert atmosphere (N_2). Column purifications were performed automatically using Biotage equipment. NMR spectra were recorded on a Bruker 300 (300 MHz), Bruker 400 (400 MHz), Bruker 500 (500 MHz), or Bruker 600 (600 MHz) spectrometer. Chemical shifts are reported in ppm (δ), and the residual solvent was used as an internal standard (δ^1H NMR: CDCl$_3$ 7.26; DMSO-d_6 2.50; CD$_3$OD 3.31; δ^{13}C NMR: CDCl$_3$ 77.16; DMSO-d_6 39.52; CD$_3$OD 49.00). Data are reported as follows: chemical shift (integration, multiplicity (s = singlet, d = doublet, t = triplet, q = quartet, br = broad signal, m = multiplet, app = apparent), and coupling constants (Hz)). A Bruker microTOF-Q mass spectrometer using ESI in positive ion mode was used to obtain HR-MS. A Shimadzu HPLC/MS workstation equipped with an Xbridge C18 5 μM column (100 mm × 4.6 mm), LC-20 AD pump system, SPD-M20A diode array detector, and LCMS-2010 EV mass spectrometer was used to perform LC−MS analyses. Almost all compounds were measured in acidic mode: the solvents that were used were the following: solvent B (acetonitrile with 0.1% formic acid) and solvent A (water with 0.1% formic acid), a flow rate of 1.0 mL/min, start 5% B, linear gradient to 90% B in 4.5 min, then 1.5 min at 90% B, then linear gradient to 5% B in 0.5 min, and then 1.5 min at 5% B; a total run time of 8 min. For occasional measuring in basic mode, the mobile phase was a mixture of A = H_2O + 10% buffer and B = MeCN +10% buffer. The buffer mentioned is a 0.4% (w/v) NH_4HCO_3 aq. soln., adjusted to pH 8.0 with aq. NH_4OH. The eluent program used is as follows: a flow rate of 1.0 mL/min, start 5% B, linear gradient to 90% B in 4.5 min, then 1.5 min at 90% B, then linear gradient to 5% B in 0.5 min, and then 1.5 min at 5% B, a total run time of 8 min. Biotage Isolera One was used for normal phase column chromatography. Reverse-phase column chromatography purifications were performed using Buchi PrepChem C-700 equipment with a discharge deuterium lamp ranging from 200 to 600 nm to detect compounds using solvent B (acetonitrile with 0.1% formic acid), solvent A (water with 0.1% formic acid), and a flow rate of 15.0 mL/min. Unless specified otherwise, all compounds have a purity of ≥95%, calculated as the percentage peak area of the analyzed compound by UV detection at 230 nm. Samples for analytical LCMS analysis were prepared by dissolving 1 mg/mL in MeCN and injecting 1 μL. The compounds in Table 2 (**10−19**) pass the PAINS filter.[42]

2-((5H-Dibenzo[a,d][7]annulen-5-yl)oxy)-N,N-dimethyle-thanamine (11). This compound was prepared as reported.[20] A mixture of 5H-dibenzo[a,d][7]annulen-5-ol (1.0 g, 4.8 mmol) and KOH (2.7 g, 48 mmol) in DMSO (9.6 mL) was stirred at room temperature. To this mixture, 2-chloro-N,N-dimethylethanamine hydrochloride (1.4 g, 9.6 mmol) was added. The mixture was stirred for 24 h at room temperature. A solution of 1.0 M aq. NaOH (13 mL) was added. The mixture was extracted with Et$_2$O (40 mL). The organic layer was dried over MgSO$_4$ and concentrated *in vacuo*. The crude product was purified by flash column chromatography (DCM/MeOH = 95:5, v/v) and reversed-phase column chromatography (H$_2$O/CH$_3$CN) to yield the title compound **11** as a yellow oil (0.10 g, 8%). High-temperature NMR: ^{1}H NMR (400 MHz, DMSO-d_6, 373 K) δ 7.62 (d, J = 7.6 Hz, 2H), 7.43−7.38 (m, 4H), 7.28 (t, J = 7.4 Hz, 2H), 7.12 (s, 2H), 4.99 (s, 1H), 3.51 (t, J = 5.0 Hz, 2H), 2.50 (app t, J = 7.2 Hz 2H), 2.18 (s, 6H). ^{13}C NMR (126 MHz, CDCl$_3$) δ 139.60, 132.74, 131.35, 128.73, 127.95, 126.42, 122.59, 79.26, 68.95, 59.28, 46.29. This ^{13}C spectrum at room temperature shows peaks for conformers, while the reported ^{1}H NMR spectrum at 373 K leads to coalescence. LC−MS (ESI): t_R = 3.38 min, 99% (area % @ 230 nm), m/z 280 [M + H]$^+$. HR-MS: C$_{19}$H$_{22}$NO calc. for [M + H]$^+$ 280.1696, found 280.1687.

5-(1-Methylpiperidin-4-yl)-10,11-dihydro-5H-dibenzo-[a,d][7]annulen-5-ol (23). To dry THF (3.0 mL), Mg turnings (0.20 g, 8.2 mmol) were added and the mixture was stirred at 50 °C. Two crystals of I$_2$ and a few drops of 1,2-dibromoethane were added. A vigorous reaction started, which subsided after a few minutes. To the reaction mixture was added 4-chloro-1-methylpiperidine (1.1 g, 8.2 mmol) in THF (7.0 mL) dropwise. The mixture was heated at reflux for 1 h to form Grignard reagent **22**. The mixture was cooled to room temperature. Then, 10,11-dihydro-5H-dibenzo[a,d][7]-annulen-5-one (1.4 g, 6.6 mmol) in THF (3.0 mL) was added portionwise. The mixture was stirred at reflux overnight. The mixture was quenched with cold 10% aq. NH$_4$Cl solution, acidified with 5 M HCl (pH 3), and extracted with DCM. The aqueous phase was made alkaline with 1.0 M aq. NaOH (20 mL) and extracted with DCM. The organic layer was dried over Na$_2$SO$_4$, filtered, and concentrated *in vacuo*. The crude product was purified by flash column chromatography (cyclohexane/EtOAc/TEA = 18:80:2, v/v/v) and recrystallized from DCM to yield the title compound as a white solid (0.40 g, 16%). ^{1}H NMR (500 MHz, CDCl$_3$) δ 7.19−7.03 (m, 8H), 3.57−3.36 (m, 3H), 3.01−2.87 (m, 2H), 2.81 (d, J = 11.1 Hz, 2H), 2.22 (s, 3H), 1.78 (app t, J = 11.5 Hz, 2H), 1.50−1.39 (m, 2H), 1.30 (app q, J = 12.4 Hz, 2H). LC−MS (ESI): t_R = 3.24 min, >99% (area % @ 230 nm), m/z 308 [M + H]$^+$.

4-(10,11-Dihydro-5H-dibenzo[a,d][7]annulen-5-ylidene)-1-methylpiperidine (13). This compound was prepared as reported.[21] A mixture of alcohol **23** (0.20 g, 0.65 mmol) and formic acid (1.0 mL, 26 mmol) was heated at 100 °C for 2 h. The mixture was cooled down to 0 °C, quenched with 2.0 M aq. NaOH (10 mL), and diluted with EtOAc. The organic phase was washed with water and brine, dried over Na$_2$SO$_4$, filtered, and concentrated *in vacuo*. The crude product was purified by flash column chromatography (cyclohexane/EtOAc = 50:50, v/v) to obtain the title compound as a white solid (51 mg, 28%). ^{1}H NMR (500 MHz, CDCl$_3$) δ 7.18−7.02 (m, 8H), 3.49−3.32 (m, 2H), 2.88−2.76 (m, 2H), 2.67−2.57 (m, 2H), 2.48−2.34 (m, 4H), 2.27 (s, 3H), 2.17−2.07 (m, 2H). ^{13}C NMR (126 MHz, CDCl$_3$) δ 140.87, 138.10, 134.79, 133.81,

129.35, 128.98, 126.91, 125.55, 57.30, 46.30, 32.59, 31.08. LC−MS (ESI): t_R = 3.63 min, >99% (area % @ 230 nm), m/z 290 [M + H]$^+$. HR-MS: C$_{21}$H$_{24}$N calc. for [M + H]$^+$ 290.1903, found 290.1899.

4-Benzhydryl-1-methylpiperidine (17).[23] To dry THF (3.0 mL), Mg turnings (0.30 g, 12 mmol) were added. The mixture was stirred at 50 °C for 10 min. One crystal of I$_2$ and 1,2-dibromoethane (0.37 g, 1.9 mmol) were added. A vigorous reaction started, which subsided after a few minutes. Then, 4-chloro-1-methylpiperidine (1.6 g, 12 mmol) in THF (4.0 mL) was added and the mixture was heated at reflux for 2 h to form Grignard reagent **22**. The mixture was cooled to room temperature and (bromomethylene)dibenzene (2.4 g, 9.7 mmol) in THF (5.0 mL) was added. The mixture was stirred for 4 h, quenched with water and extracted with toluene. The organic layer was washed with water, dried over Na$_2$SO$_4$, filtered, and concentrated *in vacuo*. The crude product was purified by flash column chromatography (cyclohexane/EtOAc/TEA = 20:78:2, v/v/v) to yield the title compound as a white solid (50 mg, 2%). ^{1}H NMR (500 MHz, CDCl$_3$) δ 7.32−7.26 (m, 8H), 7.19−7.14 (m, 2H), 3.50 (d, J = 11.0 Hz, 1H), 2.82 (app d, J = 11.8 Hz, 2H), 2.26 (s, 3H), 2.14−2.03 (m, 1H), 1.90 (app t, J = 11.9 Hz, 2H), 1.57 (app d, J = 13.4 Hz, 2H), 1.33−1.19 (m, 2H). ^{13}C NMR (126 MHz, CDCl$_3$) δ 143.95, 128.62, 128.16, 126.25, 59.04, 56.12, 46.54, 39.16, 31.59. LC−MS (ESI): t_R = 3.17 min, >99% (area % @ 230 nm), m/z 266 [M + H]$^+$. HR-MS: C$_{19}$H$_{24}$N calc. for [M + H]$^+$ 266.1903, found 266.1893.

4-(10,11-Dihydro-5H-dibenzo[a,d][7]annulen-5-yl)-1-methylpiperidine (18). To dry THF (5.0 mL), Mg turnings (0.40 g, 16 mmol) were added and the mixture was stirred at 50 °C (10 min). One crystal of I$_2$ and 1,2-dibromoethane (0.37 g, 1.9 mmol) were added. A vigorous reaction started, which subsided after a few minutes. To the mixture was added 4-chloro-1-methylpiperidine (2.7 g, 20 mmol) in THF (4.0 mL). The mixture was heated at reflux for 1 h to form Grignard reagent **22**. The mixture was cooled to room temperature, and 5-chloro-10,11-dihydro-5H-dibenzo[a,d][7]-annulene (3.00 g, 13.12 mmol) in THF (5 mL) was added. The mixture was stirred for 4 h at room temperature. The mixture was diluted with toluene. The organic phase was washed with water (2×), dried over Na$_2$SO$_4$, filtered, and evaporated under reduced pressure. The crude product was purified by reversed-phase column chromatography (H$_2$O/CH$_3$CN/HCOOH). The product fractions were concentrated and extracted with DCM/satd. aq. Na$_2$CO$_3$ solution. The organic phase was dried (MgSO$_4$) and concentrated to obtain the title compound as a white solid (25 mg, 1%). ^{1}H NMR (600 MHz, CDCl$_3$) δ 7.17−7.03 (m, 8H), 3.54−3.39 (m, 3H), 2.98−2.86 (m, 2H), 2.81 (d, J = 11.7 Hz, 2H), 2.23 (s, 3H), 2.15−2.04 (m, 1H), 1.79 (t, J = 11.3 Hz, 2H), 1.50−1.40 (m, 2H), 1.36−1.25 (m, 2H). ^{13}C NMR (151 MHz, CDCl$_3$) δ 140.46, 138.98, 131.89, 130.63, 126.78, 125.66, 61.84, 56.23, 46.42, 40.51, 33.07, 32.20. LC−MS (ESI): t_R = 3.82 min, >95% (area % @ 230 nm), m/z 292 [M + H]$^+$. HR-MS: C$_{21}$H$_{26}$N calc. for [M + H]$^+$ 292.2060, found 292.2071.

5-Bromo-5H-dibenzo[a,d][7]annulene (21). A mixture of 5H-dibenzo[a,d][7]annulen-5-ol (3.0 g, 14 mmol) and CH$_3$COBr (5.8 g, 47 mmol) in EtOAc (3.0 mL) was heated at reflux for 2 h. The resulting mixture was concentrated *in vacuo*. The residue was recrystallized from cyclohexane to yield the title compound as yellow needles (1.8 g, 46%). ^{1}H NMR (500 MHz, CDCl$_3$) δ 7.51−7.42 (m, 4H), 7.42−7.35 (m, 4H),

7.19 (s, 2H), 6.53 (s, 1H). LC−MS (ESI): t_R = 5.21 min, >78% (area % @ 230 nm), m/z 191 (benzylic cation).

4-(5H-Dibenzo[a,d][7]annulen-5-yl)-1-methylpiperidine (19).[24] To dry THF (4.0 mL), Mg turnings (0.20 g, 8.4 mmol) were added and the mixture was stirred at 50 °C (10 min). Two crystals of I_2 and 1,2-dibromoethane (0.081 g, 0.43 mmol) were added. A vigorous reaction started, which subsided after a few minutes. To the mixture was added 4-chloro-1-methylpiperidine (1.1 g, 8.4 mmol) in THF (5.2 mL) dropwise. The mixture was heated at reflux for 2 h to form Grignard reagent **22**. The mixture was cooled to room temperature. To the mixture was added bromide **21** (1.7 g, 6.3 mmol). The mixture was stirred at room temperature overnight. The mixture was quenched with water and extracted with toluene. The organic layer was washed with water, brine, dried over Na_2SO_4, filtered, and concentrated *in vacuo*. The crude product was purified by flash column chromatography (cyclohexane/EtOAc = 60:40, v/v) to obtain the title compound as a white solid (40 mg, 2%). ^1H NMR (500 MHz, $CDCl_3$) δ 7.32−7.27 (m, 4H), 7.25−7.20 (m, 4H), 6.88 (s, 2H), 3.56 (d, J = 10.7 Hz, 1H), 2.70 (app d, J = 11.4 Hz, 2H), 2.18 (s, 3H), 2.02−1.91 (m, 1H), 1.67 (t, J = 11.8 Hz, 2H), 1.21−1.08 (m, 2H), 1.03−0.96 (m, 2H). ^{13}C NMR (126 MHz, $CDCl_3$) δ 140.02, 133.93, 130.92, 130.73, 129.71, 128.54, 126.38, 61.42, 55.81, 46.37, 32.62, 31.61. LC−MS (ESI): t_R = 3.54 min, >99% (area % @ 230 nm), m/z 290 [M + H]$^+$. HR-MS: $C_{21}H_{24}N$ calc. for [M + H]$^+$ 290.1903, found 290.1911.

2-((10,11-Dihydro-5H-dibenzo[a,d][7]annulen-5-yl)oxy)-N,N-dimethylethan-1-amine maleate (10).[20] Gift from Gist Brocades (The Netherlands). ^1H NMR (500 MHz, DMSO-d_6) δ 9.29 (br, 1H), 7.40 (dd, J = 7.2, 2.1 Hz, 2H), 7.27−7.22 (m, 2H), 7.21−7.12 (m, 4H), 6.02 (s, 2H), 5.55 (s, 1H), 3.62 (t, J = 5.1 Hz, 2H), 3.48−3.40 (m, 2H), 3.29 (t, J = 5.2 Hz, 2H), 3.01−2.91 (m, 2H), 2.74 (s, 6H). ^{13}C NMR (126 MHz, DMSO-d_6) δ 167.20, 139.14, 137.98, 136.17, 130.29, 128.74, 128.31, 125.90, 83.98 (confirmed by HSQC), 62.73, 55.94, 42.74, 31.45. LC−MS (ESI): t_R = 3.49 min, >99% (area % @ 230 nm), m/z 282 [M + H]$^+$. HR-MS: $C_{19}H_{24}NO$ calc. for [M + H]$^+$ 282.1852, found 282.1845.

4-(Diphenylmethylene)-1-methylpiperidine Hydrochloride (12).[21] Gift from Gist Brocades (The Netherlands). ^1H NMR (500 MHz, DMSO-d_6) δ 10.59 (s, 1H), 7.38−7.32 (m, 4H), 7.29−7.23 (m, 2H), 7.16−7.09 (m, 4H), 3.49−3.37 (m, 2H), 3.10−2.95 (m, 2H), 2.73 (s, 3H), 2.53−2.50 (m, 4H). ^{13}C NMR (126 MHz, DMSO-d_6) δ 141.2, 138.0, 129.2, 129.0, 128.4, 127.0, 53.9, 42.2, 28.1. LC−MS (ESI): t_R = 3.48 min, >99% (area % @ 230 nm), m/z 264 [M + H]$^+$ HR-MS: $C_{19}H_{22}N$ calc. for [M + H]$^+$ 264.1747, found 264.1758.

1-(10,11-Dihydro-5H-dibenzo[a,d][7]annulen-5-yl)-4-methylpiperazine (15).[22] Gift from Gist Brocades (The Netherlands). ^1H NMR (500 MHz, DMSO-d_6) δ 7.21−7.17 (m, 2H), 7.15 (dd, J = 7.3, 1.4 Hz, 2H), 7.13−7.10 (m, 2H), 7.09−7.04 (m, 2H), 4.00 (s, 1H), 3.95−3.83 (m, 2H), 2.78−2.68 (m, 2H), 2.51 (s, 3H), 2.44−1.78 (m, 8H). ^{13}C NMR (126 MHz, DMSO-d_6) δ 139.31, 139.00, 130.65, 130.43, 127.68, 125.52, 77.78, 54.99, 51.40, 45.71, 30.98. LC−MS (ESI): t_R = 3.48 min, >99% (area % @ 230 nm), m/z 293 [M + H]$^+$. HR-MS: $C_{20}H_{25}N_2$ calc. for [M + H]$^+$ 293.2012, found 293.2004.

1-(5H-Dibenzo[a,d][7]annulen-5-yl)-4-methylpiperazine (16).[21] Gift from Gist Brocades (The Netherlands). ^1H NMR (500 MHz, DMSO-d_6) δ 7.48−7.39 (m, 4H), 7.39−7.25 (m,

4H), 6.97 (s, 2H), 4.34 (s, 1H), 2.12−1.68 (br m, 11H). ^{13}C NMR (126 MHz, DMSO-d_6) δ 137.95, 134.08, 130.32, 129.92, 129.44, 128.09, 127.05, 76.68, 54.47, 51.05, 45.62. LC−MS (ESI): t_R = 5.49 min, >99% (area % @ 230 nm, basic mode), m/z 291 [M + H]$^+$. HR-MS: $C_{20}H_{23}N_2$ calc. for [M + H]$^+$ 291.1856, found 191.0879 (benzylic cation).

4-(5H-Dibenzo[a,d][7]annulen-5-ylidene)-1-methylpiperidine Hydrochloride (14).[25] Gift from Gist Brocades (The Netherlands). ^1H NMR (400 MHz, DMSO-d_6) δ 10.34 (br s, 1H), 7.46−7.38 (m, 4H), 7.36−7.29 (m, 2H), 7.29−7.23 (m, 2H), 7.00 (s, 2H), 3.35−3.20 (br, 4H), 2.68 (br s, 3H), 2.58−2.47 (br, 2H), 2.38−2.06 (br, 2H). ^{13}C NMR (126 MHz, $CDCl_3$) δ 137.59, 137.55, 137.44, 134.69, 134.44, 131.06, 130.98, 128.88, 128.50, 128.21, 128.15, 128.04, 127.23, 127.19, 127.11, 55.80, 55.39, 43.69, 42.95, 26.84, 26.59. All ^{13}C peaks for both conformers are listed. Conformers are known for this compound in NMR analysis in $CDCl_3$.[43] LC−MS (ESI): t_R = 3.65 min, >99% (area % @ 230 nm), m/z 288 [M + H]$^+$. HR-MS: $C_{21}H_{21}N$ calc. for [M + H]$^+$ 288.1747, found 288.1749.

■ ASSOCIATED CONTENT

ⓢ Supporting Information

The Supporting Information is available free of charge at https://pubs.acs.org/doi/10.1021/acsomega.0c06358.

> Molecular formula strings (XLSX)
>
> Correlations between binding kinetics and numbers of conformers for Table 2 compounds and $^1H/^{13}C$ NMR spectroscopy data and LC−MS chromatograms for 10−19 (PDF)

■ AUTHOR INFORMATION

Corresponding Author

Iwan J.P. de Esch − *Amsterdam Institute of Molecular and Life Sciences (AIMMS), Division of Medicinal Chemistry, Faculty of Science, Vrije Universiteit Amsterdam, 1081 HZ Amsterdam, The Netherlands;* ⓞ orcid.org/0000-0002-1969-0238; Phone: +31 20 5987841; Email: i.de.esch@vu.nl

Authors

Zhiyong Wang − *Amsterdam Institute of Molecular and Life Sciences (AIMMS), Division of Medicinal Chemistry, Faculty of Science, Vrije Universiteit Amsterdam, 1081 HZ Amsterdam, The Netherlands*

Reggie Bosma − *Amsterdam Institute of Molecular and Life Sciences (AIMMS), Division of Medicinal Chemistry, Faculty of Science, Vrije Universiteit Amsterdam, 1081 HZ Amsterdam, The Netherlands*

Sebastiaan Kuhne − *Amsterdam Institute of Molecular and Life Sciences (AIMMS), Division of Medicinal Chemistry, Faculty of Science, Vrije Universiteit Amsterdam, 1081 HZ Amsterdam, The Netherlands*

Jelle van den Bor − *Amsterdam Institute of Molecular and Life Sciences (AIMMS), Division of Medicinal Chemistry, Faculty of Science, Vrije Universiteit Amsterdam, 1081 HZ Amsterdam, The Netherlands*

Wrej Garabitian − *Amsterdam Institute of Molecular and Life Sciences (AIMMS), Division of Medicinal Chemistry, Faculty of Science, Vrije Universiteit Amsterdam, 1081 HZ Amsterdam, The Netherlands*

Henry F. Vischer − *Amsterdam Institute of Molecular and Life Sciences (AIMMS), Division of Medicinal Chemistry,*

Faculty of Science, Vrije Universiteit Amsterdam, 1081 HZ Amsterdam, The Netherlands; ● orcid.org/0000-0002-0184-6337

Maikel Wijtmans − *Amsterdam Institute of Molecular and Life Sciences (AIMMS), Division of Medicinal Chemistry, Faculty of Science, Vrije Universiteit Amsterdam, 1081 HZ Amsterdam, The Netherlands;* ● orcid.org/0000-0001-8955-8016

Rob Leurs − *Amsterdam Institute of Molecular and Life Sciences (AIMMS), Division of Medicinal Chemistry, Faculty of Science, Vrije Universiteit Amsterdam, 1081 HZ Amsterdam, The Netherlands;* ● orcid.org/0000-0003-1354-2848

Complete contact information is available at:
https://pubs.acs.org/10.1021/acsomega.0c06358

Author Contributions

#Z.W., R.B., and S.K. have equal contribution.

Notes

The authors declare no competing financial interest.

■ ABBREVIATIONS

THF, tetrahydrofuran; TEA, triethylamine; DCM, dichloromethane; DMSO, dimethylsulfoxide; GPCR, G protein-coupled receptor; H_1R, histamine H_1 receptor; SAR, structure−affinity relationship; SKR, structure−kinetics relationship; RT, residence time

■ REFERENCES

(1) Hoffmann, C.; Castro, M.; Rinken, A.; Leurs, R.; Hill, S. J.; Vischer, H. F. Ligand Residence Time at G-protein−Coupled Receptors—Why We Should Take Our Time To Study It. *Mol. Pharmacol.* **2015**, *88*, 552−560.

(2) Swinney, D. C. Biochemical mechanisms of drug action: what does it take for success? *Nat. Rev. Drug Discov.* **2004**, *3*, 801−808.

(3) Copeland, R. A. The drug−target residence time model: A 10-year retrospective. *Nat. Rev. Drug Discov.* **2015**, *15*, 87−95.

(4) Lu, H.; Tonge, P. J. Drug−target residence time: Critical information for lead optimization. *Curr. Opin. Chem. Biol.* **2010**, *14*, 467−474.

(5) Guo, D.; Mulder-Krieger, T.; Ijzerman, P. A.; Heitman, H. L. Functional efficacy of adenosine A2A receptor agonists is positively correlated to their receptor residence time. *Br. J. Pharmacol.* **2012**, *166*, 1846−1859.

(6) Gillard, M.; Van Der Perren, C.; Moguilevsky, N.; Massingham, R.; Chatelain, P. Binding characteristics of cetirizine and levocetirizine to human H1 histamine receptors: Contribution of Lys191 and Thr194. *Mol. Pharmacol.* **2002**, *61*, 391−399.

(7) Guo, D.; IJzerman, A. P., Molecular basis of ligand dissociation from G protein-coupled receptors and predicting residence time. In *Computational Methods for GPCR Drug Discovery*, 1ˢᵗ ed.; Heifetz, A., Ed.; Humana Press: Totowa, 2018; pp 197−206.

(8) Tautermann, C. S.; Kiechle, T.; Seeliger, D.; Diehl, S.; Wex, E.; Banholzer, R.; Gantner, F.; Pieper, M. P.; Casarosa, P. Molecular basis

(9) Miller, D. C.; Lunn, G.; Jones, P.; Sabnis, Y.; Davies, N. L.; Driscoll, P. Investigation of the effect of molecular properties on the binding kinetics of a ligand to its biological target. *MedChemComm.* **2012**, *3*, 449−452.

(10) Pan, A. C.; Borhani, D. W.; Dror, R. O.; Shaw, D. E. Molecular determinants of drug−receptor binding kinetics. *Drug Discovery Today* **2013**, *18*, 667−673.

(11) Tresadern, G.; Bartolome, J. M.; Macdonald, G. J.; Langlois, X. Molecular properties affecting fast dissociation from the D2 receptor. *Bioorg. Med. Chem.* **2011**, *19*, 2231−2241.

(12) Veber, D. F.; Johnson, S. R.; Cheng, H.-Y.; Smith, B. R.; Ward, K. W.; Kopple, K. D. Molecular properties that influence the oral bioavailability of drug candidates. *J. Med. Chem.* **2002**, *45*, 2615−2623.

(13) Schmidtke, P.; Luque, F. J.; Murray, J. B.; Barril, X. Shielded hydrogen bonds as structural determinants of binding kinetics: Application in drug design. *J. Am. Chem. Soc.* **2011**, *133*, 18903−18910.

(14) Bosma, R.; Moritani, R.; Leurs, R.; Vischer, H. F. BRET-based β-arrestin2 recruitment to the histamine H1 receptor for investigating antihistamine binding kinetics. *Pharmacol. Res.* **2016**, *111*, 679−687.

(15) Bosma, R.; Witt, G.; Vaas, L. A. I.; Josimovic, I.; Gribbon, P.; Vischer, H. F.; Gul, S.; Leurs, R. The target residence time of antihistamines determines their antagonism of the G protein-coupled histamine H1 receptor. *Front. Pharmacol.* **2017**, *8*, 667.

(16) Anthes, J. C.; Gilchrest, H.; Richard, C.; Eckel, S.; Hesk, D.; West Jr, R. E.; Williams, S. M.; Greenfeder, S.; Billah, M.; Kreutner, W.; Egan, R. W. Biochemical characterization of desloratadine, a potent antagonist of the human histamine H1 receptor. *Eur. J. Pharmacol.* **2002**, *449*, 229−237.

(17) Gillard, M.; Chatelain, P. Changes in pH differently affect the binding properties of histamine H1 receptor antagonists. *Eur. J. Pharmacol.* **2006**, *530*, 205−214.

(18) Bosma, R.; Stoddart, L. A.; Georgi, V.; Bouzo-Lorenzo, M.; Bushby, N.; Inkoom, L.; Waring, M. J.; Briddon, S. J.; Vischer, H. F.; Sheppard, R. J.; Fernández-Montalván, A.; Hill, S. J.; Leurs, R. Probe dependency in the determination of ligand binding kinetics at a prototypical G protein-coupled receptor. *Sci. Rep.* **2019**, *9*, 7906.

(19) Kuhne, S.; Kooistra, A. J.; Bosma, R.; Bortolato, A.; Wijtmans, M.; Vischer, H. F.; Mason, J. S.; de Graaf, C.; de Esch, I. J. P.; Leurs, R. Identification of ligand binding hot spots of the histamine H1 receptor following structure-based fragment optimization. *J. Med. Chem.* **2016**, *59*, 9047−9061.

(20) Van Der Stelt, C.; Harms, A. F.; Nauta, W. T. The effect of alkyl-substitution in drugs–V. Synthesis and chemical properties of some dibenzo [a,d]1,4-cycloheptadienyl ethers. *J. Med. Pharm. Chem.* **1961**, *4*, 335−349.

(21) Fujiwara, T.; Ohira, K.; Urushibara, K.; Ito, A.; Yoshida, M.; Kanai, M.; Tanatani, A.; Kagechika, H.; Hirano, T. Steric structure−activity relationship of cyproheptadine derivatives as inhibitors of histone methyltransferase Set7/9. *Bioorg. Med. Chem.* **2016**, *24*, 4318−4323.

(22) Naporra, F.; Gobleder, S.; Wittmann, H.-J.; Spindler, J.; Bodensteiner, M.; Bernhardt, G.; Hübner, H.; Gmeiner, P.; Elz, S.; Strasser, A. Dibenzo[b,f][1,4]oxazepines and dibenzo[b,e]oxepines: Influence of the chlorine substitution pattern on the pharmacology at the H_1R, H_4R, 5-HT2AR and other selected GPCRs. *Pharmacol. Res.* **2016**, *113*, 610−625.

(23) Ismaiel, A. M.; Arruda, K.; Teitler, M.; Glennon, R. A. Ketanserin Analogs: The effect of structural modification on 5-HT2 serotonin receptor binding. *J. Med. Chem.* **1995**, *38*, 1196−1202.

(24) Young, S. D.; Baldwin, J. J.; Cochran, D. W.; King, S. W.; Remy, D. C.; Springer, J. P. Conformational mobility of dibenzo[a,d]-cycloheptene derivatives. Preparation and characterization of two intraconverting conformational isomers. *J. Org. Chem.* **1985**, *50*, 339−342.

(25) Wolf, C.; Schunack, W. Synthesis and pharmacology of combined histamine H1-/H2-receptor antagonists containing diphenhydramine and cyproheptadine derivatives. *Arch. Pharm.* **1996**, *329*, 87−94.

(26) Taylor, B. L. H.; Harris, M. R.; Jarvo, E. R. Synthesis of enantioenriched triarylmethanes by stereospecific cross-coupling reactions. *Angew. Chem., Int. Ed.* **2012**, *51*, 7790−7793.

(27) Kawamura, Y.; Iwano, Y.; Watanabe, N.; Horie, T.; Tsukayama, M. Reactivity of methylenetriphenylphosphoranes having two phenyl groups constrained with ethano or etheno bridge. *Phosphorus, Sulfur Silicon Relat. Elem.* **1998**, *132*, 167−181.

(28) Engelhardt, E. L.; Zell, H. C.; Saari, W. S.; Christy, M. E.; Colton, C. D.; Stone, C. A.; Stavorski, J. M.; Wenger, H. C.; Ludden, C. T. Structure-activity relationships in the cyproheptadine series. *J. Med. Chem.* **1965**, *8*, 829−835.

(29) Motulsky, H. J.; Mahan, L. C. The kinetics of competitive radioligand binding predicted by the law of mass action. *Mol. Pharmacol.* **1984**, *25*, 1−9.

(30) Bosma, R.; Mocking, T.; Leurs, R.; Vischer, H., Ligand-binding kinetics on histamine receptors, Histamine Receptors as Drug Targets. In *Method in Pharmacology and Toxicology*; Tiligada, E.; Ennis, M., Ed.; Humana Press: New York, 2017; pp. 115−155.

(31) Bosma, R.; Wang, Z.; Kooistra, A. J.; Bushby, N.; Kuhne, S.; van den Bor, J.; Waring, M. J.; de Graaf, C.; de Esch, I. J.; Vischer, H. F.; Sheppard, R. J.; Wijtmans, M.; Leurs, R. Route to prolonged residence time at the histamine H1 receptor: Growing from desloratadine to rupatadine. *J. Med. Chem.* **2019**, *62*, 6630−6644.

(32) Simons, F. E. R.; Simons, K. J. Histamine and H1-antihistamines: Celebrating a century of progress. *J.Allergy Clin. Immunol.* **2011**, *128*, 1139−1150.e4.

(33) Simons, F. E. R. Advances in H1-antihistamines. *New. Engl. J. Med.* **2004**, *351*, 2203−2217.

(34) Parsons, M. E.; Ganellin, C. R. Histamine and its receptors. *Br. J. Pharmacol.* **2006**, *147*, S127−S135.

(35) Huang, Z.-L.; Mochizuki, T.; Qu, W.-M.; Hong, Z.-Y.; Watanabe, T.; Urade, Y.; Hayaishi, O. Altered sleep−wake characteristics and lack of arousal response to H3 receptor antagonist in histamine H1 receptor knockout mice. *Proc. Natl. Acad. Sci. U. S. A.* **2006**, *103*, 4687−4692.

(36) Ikeda-Sagara, M.; Ozaki, T.; Shahid, M.; Morioka, E.; Wada, K.; Honda, K.; Hori, A.; Matsuya, Y.; Toyooka, N.; Ikeda, M. Induction of prolonged, continuous slow-wave sleep by blocking cerebral H1 histamine receptors in rats. *Br. J. Pharmacol.* **2012**, *165*, 167−182.

(37) Parmentier, R.; Zhao, Y.; Perier, M.; Akaoka, H.; Lintunen, M.; Hou, Y.; Panula, P.; Watanabe, T.; Franco, P.; Lin, J.-S. Role of histamine H1-receptor on behavioral states and wake maintenance during deficiency of a brain activating system: A study using a knockout mouse model. *Neuropharmacology* **2016**, *106*, 20−34.

(38) Xia, L.; Burger, W. A. C.; van Veldhoven, J. P. D.; Kuiper, B. J.; van Duijl, T. T.; Lenselink, E. B.; Paasman, E.; Heitman, L. H.; Ijzerman, A. P. Structure−affinity relationships and structure−kinetics relationships of pyrido[2,1-f]purine-2,4-dione derivatives as human adenosine A3 receptor antagonists. *J. Med. Chem.* **2017**, *60*, 7555−7568.

(39) Xia, L.; Kyrizaki, A.; Tosh, D. K.; van Duijl, T. T.; Roorda, J. C.; Jacobson, K. A.; Ijzerman, A. P.; Heitman, L. H. A binding kinetics study of human adenosine A3 receptor agonists. *Biochem. Pharmacol.* **2018**, *153*, 248−259.

(40) Mocking, T. A. M.; Verweij, E. W. E.; Vischer, H. F.; Leurs, R. Homogeneous, real-time nanoBRET binding assays for the histamine H3 and H4 receptors on living cells. *Mol. Pharmacol.* **2018**, *94*, 1371−1381.

(41) Yung-Chi, C.; Prusoff, W. H. Relationship between the inhibition constant (KI) and the concentration of inhibitor which causes 50 per cent inhibition (I50) of an enzymatic reaction. *Biochem. Pharmacol.* **1973**, *22*, 3099−3108.

(42) Baell, J. B.; Holloway, G. A. New substructure filters for removal of pan assay interference compounds (PAINS) from screening libraries and for their exclusion in bioassays. *J. Med. Chem.* **2010**, *53*, 2719−2740.

(43) Sadek, M.; Craik, D. J.; Hall, J. G.; Andrews, P. R. Conformational analysis of cyproheptadine hydrochloride. *J. Med. Chem.* **1990**, *33*, 1098−1107.